Title

Site-laboratory investigation strategies to characterize a complex slope instability phenomenon in Southern Italy

Journal

ITALIAN GEOTECHNICAL JOURNAL-RIVISTA ITALIANA DI GEOTECNICA, 55(4)

ISSN

0557-1405

Authors

Ausilio, Ernesto
Zimmaro, Paolo

Publication Date

2021

DOI

10.19199/2021.4.0557-1405.032

Site-laboratory investigation strategies to characterize a complex slope instability phenomenon in Southern Italy

Ernesto Ausilio[1] and Paolo Zimmaro[2,3]

[1] Department of Civil Engineering, University of Calabria, Rende, Italy
[2]Department of Environmental Engineering, University of Calabria, Rende, Italy
[3] Department of Civil and Environmental Engineering, University of California, Los Angeles, USA
ernesto.ausilio@unical.it
paolo.zimmaro@unical.it

Abstract. Slopes instabilities are complex phenomena and constitute a major hazard for human activities.Slope instabilities affect most of the countries overlooking the Mediterranean Sea and often involve challenging geotechnical conditions and complex geo-material characteristics. In this paper we present a combined field-laboratory multidisciplinary test and monitoring program to characterize slope instability phenomena in the town of Gimigliano (Southern Italy). These phenomena involve complex geo-morphological aspects and the interaction of several landslides with different dimensions and characteristics. The study area is located on the east coast of the Calabria region, in Southern Italy, within the narrow Calabrian Arc subduction zone, where sections of the oceanic plate (one of the oldest in the world) have been thrusted and preserved on land. The area is characterized by the so-called Liguride and Calabride complexes and the presence of Mesozoic ophiolitic rocks.
During the period 2008-2010, this area was affected by persistent rainfall events which reactivated various landslides causing damage to buildings and infrastructure systems. To characterize this complex slope instability phenomenon a comprehensive site and laboratory test and monitoring program has been performed. We gathered information on: (1) tectonic, geological and geomorphological background, (2) hydrogeological conditions, (3) evolution over time and space of the activity by monitoring techniques such as multi-epoch Synthetic Aperture Radar (SAR), inclinometer, and structural monitoring, (4) geotechnical characteristics from boring logs and standard laboratory tests, (5) spatial distribution and variation of geologic units via electrical resistivity tomography, (6) geotechnical field monitoring, and (7) advanced laboratory ultrasonic testing on samples retrieved in the unstable area for the determination of P and Swave velocities. This comprehensive multidisciplinary characterization allowed us to understand the complexity of this phenomenon, gaining insights into issues pertaining to slope instabilities in similar geologic and tectonic environments in the Calabria region and in the whole Mediterranean area.

Keywords: Complex geo-material characteristics, Field and laboratory investigation, Multidisciplinary characterization, Ultrasonic testing.

1. Introduction

The characterization of complex slope instability phenomena involves multiple factors and it is, as a result, a very difficult, while essential task to be performed. According to Travelletti and Malet [2012], five information types, involving both material characterization and monitoring strategies, are required to obtain an adequate level of knowledge about landslides: (a) kinematic data (*i.e.* activity and distribution of velocities), (b) geomorphologic information (*i.e.* landform type), (c) geological characterization (*i.e.* the geologic units involved), (d) geotechnical characterization (*i.e.* geomechanical and strength characterization), and (e) petrophysical information (*i.e.* physical-chemical information of the rocks involved). Ideally, landslide characterization efforts would be based on all five information types. However, such an ideal characterization strategy is often impractical or too expensive/time consuming. In recent years several characterization approaches were proposed for different landslide types and adopting various techniques and tools [*e.g.*, Agnesi *et al.*, 2005; Mantovani *et al.*, 2013; Ausilio and Zimmaro, 2017; Tomás *et al.*, 2018; Pastor *et al.*, 2019; Bentivenga *et al.*, 2019 and 2021]. Along with material characterization approaches and tools, a very important element for a good characterization of complex landslides is represented by the

evolution over time and space of the activity by monitoring techniques. Such monitoring strategies may be performed using various tools, including damage surveys (typically used as a complementary technique to traditional monitoring tools [*e.g.*, Notti *et al.*, 2015; Del Soldato *et al.*, 2017, Tomas *et al.*, 2018]. These damage assessments are particularly useful in urban areas, where cracks can be accurately measured. Therefore, a detailed analysis of damage affecting structures and infrastructures can complement and enhance the level of knowledge of such phenomena, ultimately yielding useful information on the kinematic characteristics of the landslide [Tomas *et al.*, 2018; Del Soldato *et al.*, 2018].

In this study we analyze the town of Gimigliano (Southern Italy) which is affected by the presence of several instability phenomena that are characterized by different types of landslides with different states, distributions, and styles of activity. This complexity is mainly related to a heterogeneous geologic setting and the presence of active tectonic structures. Such instability phenomena were monitored using remote-sensing techniques that showed, over the years, a clear general deformation pattern with acute and intense phases alternated with more moderate phases [*i.e.*, Ausilio and Zimmaro, 2017]. The most recent intense deformation phase occurred in February 2010, causing substantial damage to roadways and buildings. Such deformations were mainly caused by a deep-seated landslide phenomenon. Following this deformation phase, local officials funded a field-laboratory investigation program aiming at facilitating the implementation of landslide risk mitigation strategies. In this paper we describe how the combination of various direct and indirect site-laboratory investigation and monitoring techniques were used to characterize the complex instability phenomena affecting the municipality of Gimigliano.

2. The Gimigliano landslide

2.1 Tectonic, geological, and geomorphological background

The village of Gimigliano is located in the Calabria region (Southern Italy). The upper part of the town (*Gimigliano superiore*) is located on sloping ridges of the *Gimigliano Mountain*. This area can be subdivided into two zones: the medieval village and a new building estate (Figs. 1 and 2).

Gimigliano is located within the narrow Calabrian Arc subduction zone where the Ionian ocean crust of the African plate subduces the Eurasian continental plate. As part of this complex mechanism, within the accretionary wedge of this tectonic feature (*i.e.*, the prismatic shaped area at the boundary between plates where accreted sediments accumulate) sections of the oceanic plate (one of the oldest in the world), known as ophiolites, are appeneded to the continental crust and preserved on land. This phenomenon occurs when portions of the oceanic crust break away from the subducting slab as it descends and instead of being subducted, they are thrusted (*i.e.*, moved over) the overriding plate (*i.e.*, obducted).As a result, the area is characterized by the presence of both: oceanic-derived ophiolitic rocks (*i.e.*, the Liguride complex) and continental units (*i.e.*, the Calabrian complex). The Gimigliano ophiolite outcrops consist of metabasite and serpentinite [Colonna and Piccarreta, 1975, 1977; Rossetti *et al.*, 2001].

As shown in Fig. 3, the area is characterized by the presence of a variety of shallow tectonic features including the regional NW-SE-trending left-lateral strike-slip fault system, developed between the southern edge of the Crati Valley area (*i.e.*, a graben lying between two norma fault system)and the Catanzaro Trough (*i.e.*, a Neogene-Quaternary sedimentary basin) . This system consists of three right-stepping *en-echelon* major faults, from North to South (Fig. 3a): the Falconara-Carpanzano Fault", the Amantea-Gimigliano Fault, and the Lamezia-Catanzaro Fault (partially buried in the Eastern side). These faults are characterized by well-developed escarpments, with triangular and/or trapezoidal facets, and control the drainage network. Gimigliano lies between two overalapping areas between these faults. Interestingly, in the area between the Amantea-Gimigliano fault and Lamezia-Catanzaro fault, contractional tectonic deformations produced the push-ups of Mt. Reventino and the Gimigliano area; thus determining the characteristic topography where the town of Gimigliano is built. In particular, the Gimigliano push-up developed between the Amantea-Gimigliano fault and a minor left-lateral strike-slip fault extending from Gimigliano Inferiore to Cavorà, a hamlet SE of

Gimigliano [Fig. 3b; Tansi *et al.*, 2007]. These tectonic features generate many cataclastic zones characterized by weathered and intensively fractured rocks. The outcropping rocks show a stone behavior, even if schistosity and jointing lead to the formation of deep granular and highly erodible layers. [Filomena 2019]. This geologic complexity is evident in Fig. 3a.

Fig. 4 shows the landslide inventory map produced by the Calabria Region [*Piano per l'Assetto Idrogeologico*, PAI, 2016] for the Gimigliano area. In this map, it is evident that the new building estate is affected by a complex phenomenon of instability, known as the *Gimigliano landslide*. This complex phenomenon involves minor landslides overlapping, and in some areas covering, the main body of the landslide. As shown in Fig. 4 6, the main body of the landslide extends for a length of about 1300 m and for a width of about 800 m and has a well identified right flank and a less evident left flank for the presence of minor instabilities. It is set on a substrate consisting of metamorphic units (ophiolitic rocks) and philladic schists belonging to the Jurassic and to the Upper Oligocene Frido Unit (an ocean-continent transition zone). The top part of the landslide does not show morphological signs of recent activity and the various morphological steps and escarpments correspond in part to morphoselection escarpments (phyllite-metacalcari) and in part to landslides escarpments remodeled and covered with vegetation to testify the inactivity of this portion of the slope. The old landslide body is affected by morphological escarpments which, although disjointed, constitute the recent Gimigliano landslide. The escarpments are clear and arched in the area upstream of the Corace river while they gradually become less pronounced towards the east. The central part of the Gimigliano landslide is characterized by a variety of different movement components and a certain complexity in its historical evolution (Fig. 4). The lower middle part of the slope consists of an accumulation of metamorphic material, sometimes chaotic and immersed in a fine matrix that constitutes the accumulation of the landslide. It appears to be the product of the evolution of translational flows with a rotational component mainly evolved or covered by debris flows or debris avalanches that probably did not reach, at least in its most recent part, the current Corace riverbed.

The basic stratigraphic sequence in the Gimigliano area comprises phyllites, metarenites and metaconglomerates intercalated by metalimestones overlaying banks of metabasites alternated with serpentinites and ophicalcites that are part the Mesozoic Ophiolitic unit of the Reventino Mountain (located north-west of Gimigliano) [Amodio Morelli *et al.*, 1976; Messina *et al.*, 1994; Tansi *et al.*, 2007]. Such complex stratigraphy can be summarized as a shallower detrital colluvial deposit of alteration with variable thickness that overlies the materials of the Frido Unit that includes metamorphic ophiolitic rocks and philladic schists as shown in Fig. 3a.

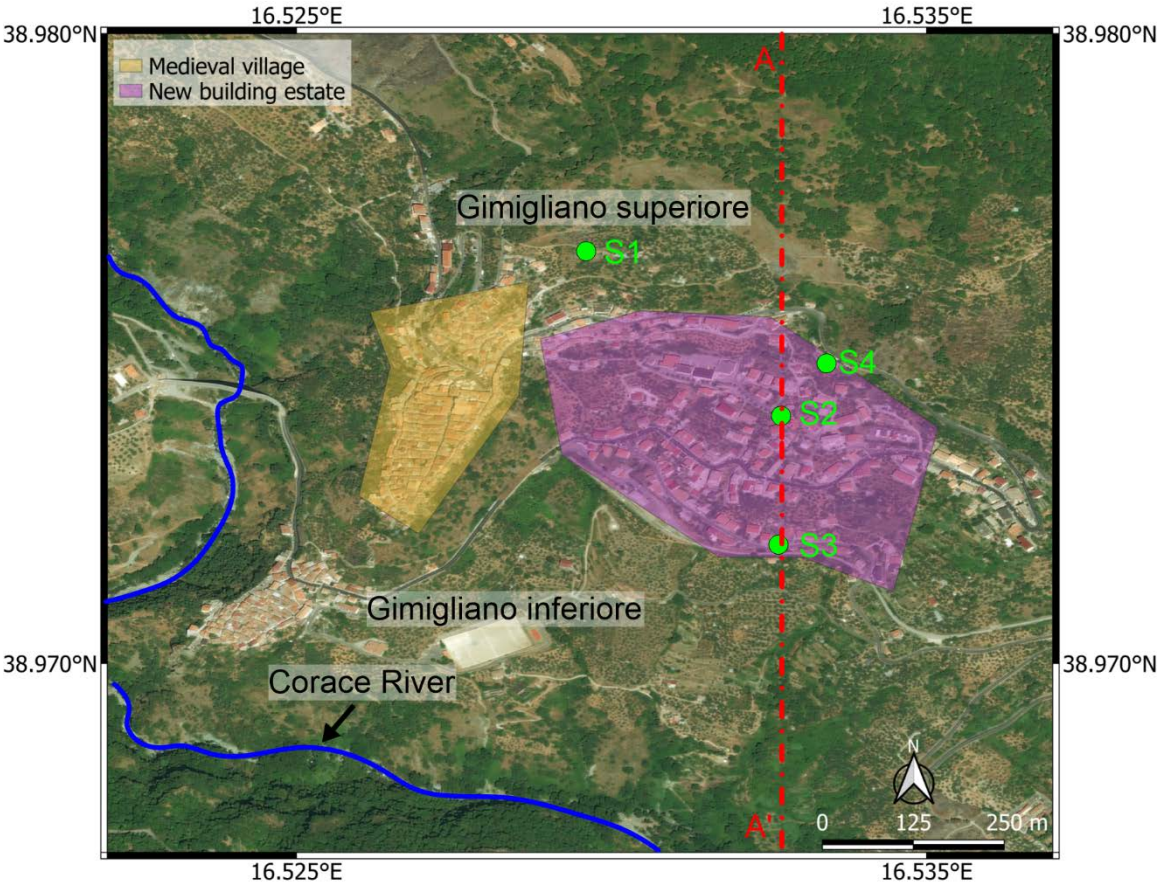

Figure 1. Plan view of the town of Gimigliano.

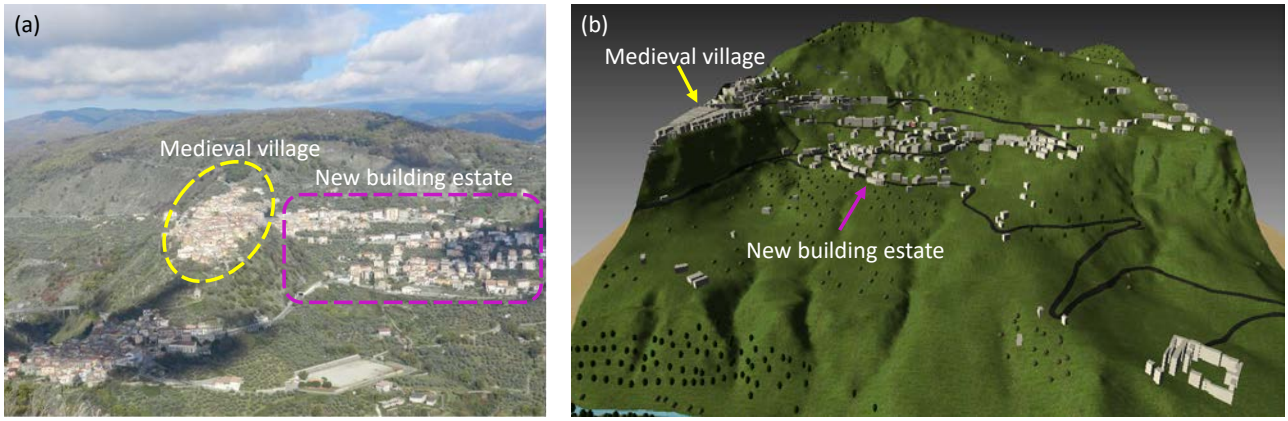

Figure 2. (a) Aerial view of Gimigliano; (b) 3D model of Gimigliano.

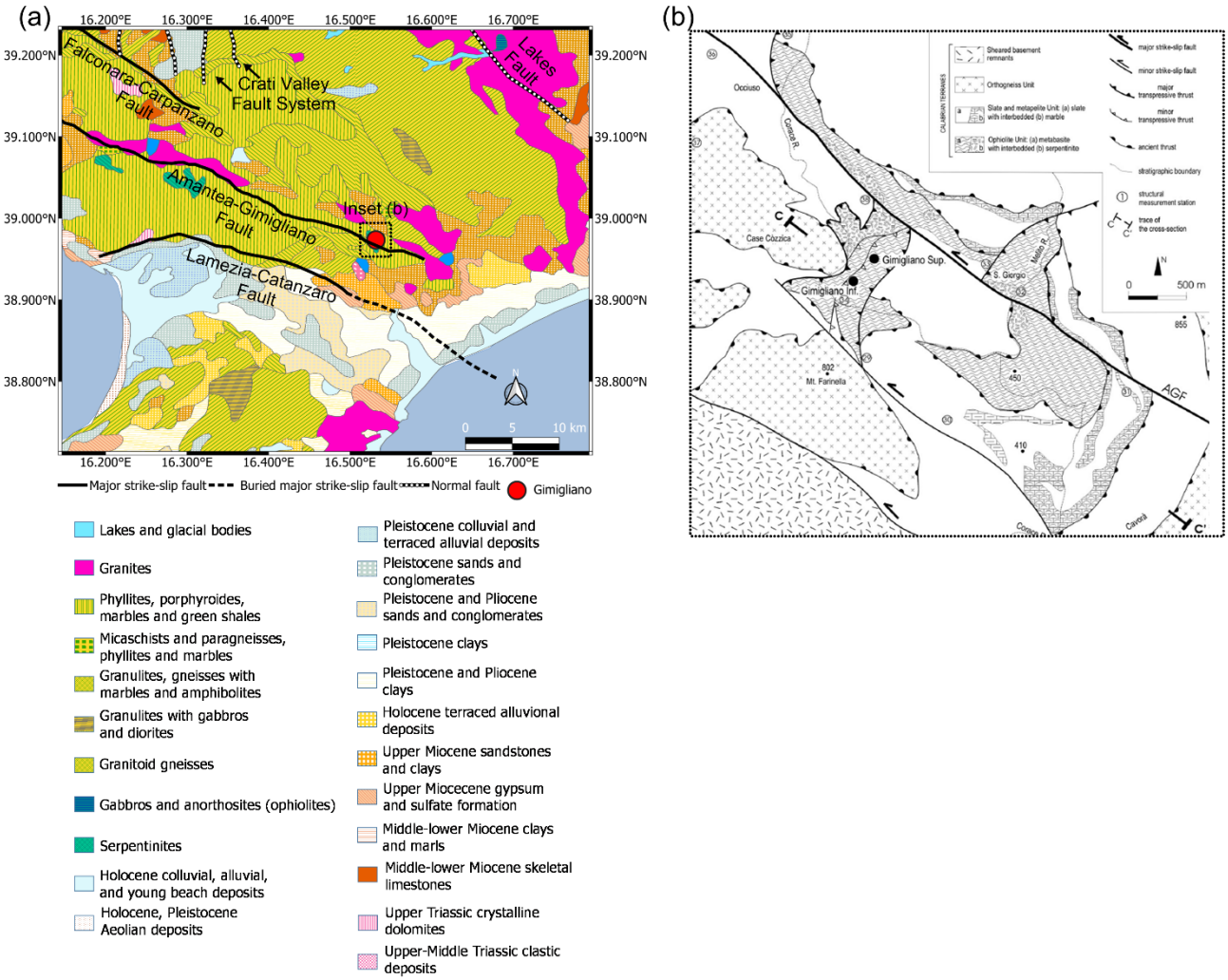

Figure 3. (a) Geology map with main seismogenic fault systems of Central Calabria [fault geometries are from Tansi *et al.*, 2007: Crati Valley, Falconara-Carpanzano, Amantea-Gimigliano, and Lamezia-Catanzaro) and Zimmaro and Stewart, 2016; Lakes]; (b) Zoomed-in structural map of Gimigliano [adapted from Tansi *et al.*, 2007].

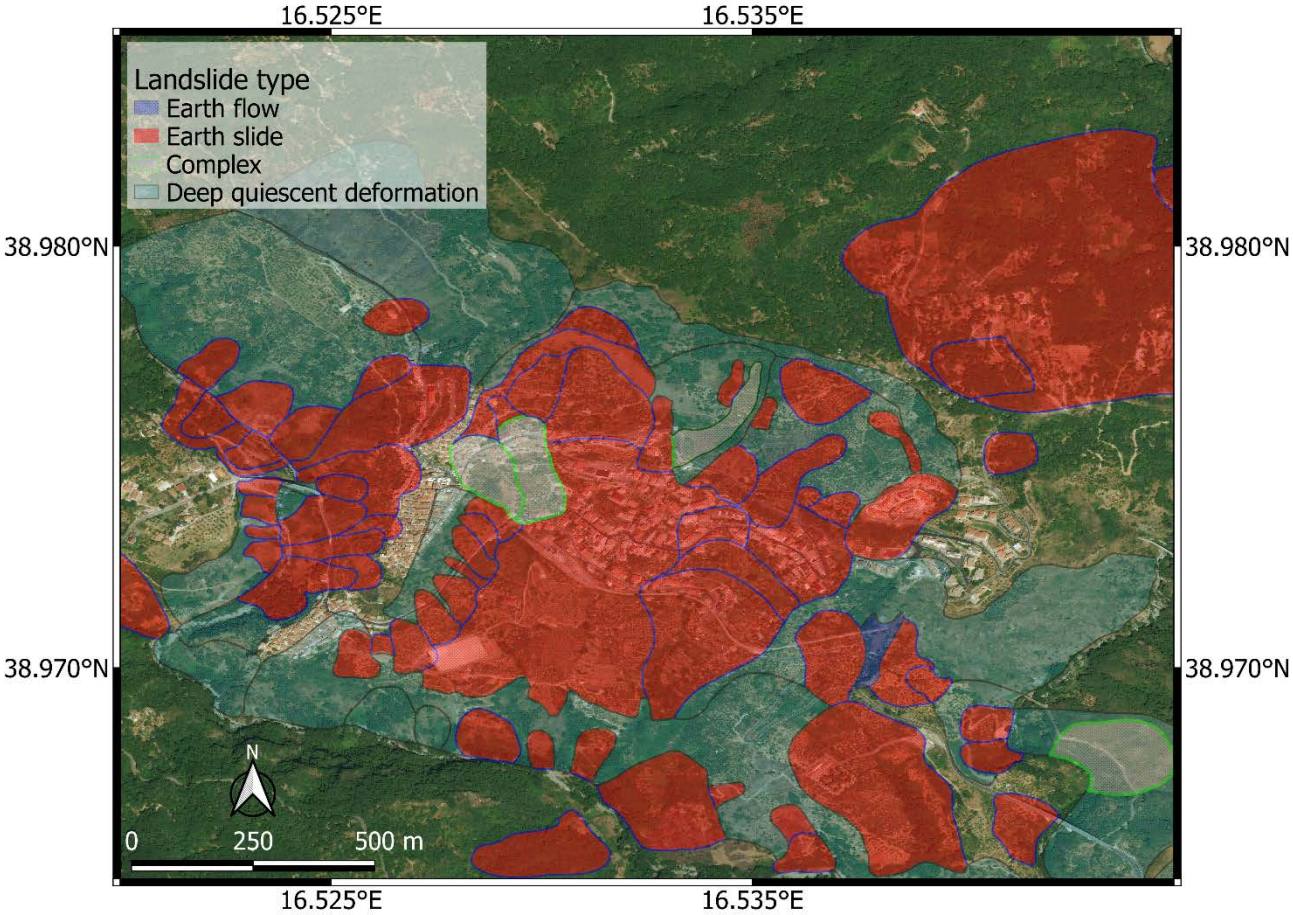

Figure 4. Mapped landslides in thGimigliano area [landslide inventory data from PAI, 2016].

2.2 hydrogeological conditions

The area of Gimigliano is characterized by a highly developed drainage system, consisting of numerous ditches and incisions flowing into the main stream of the area: the Corace river. Such complex drainage system affects the southern slope of the Gimigliano Mountain and includes the area occupied by the Gimigliano landslide. Hydrogeologically, the philladic schist and fractured green schist formations constitute an aquifer complex with relatively high permeability. At different depths, the same formations, if intact, constitutes the impermeable substrate of the aquifer. Within the shallower detrital colluvial deposit of alteration, which covers the schistous metamorphic substrate with highly variable thicknesses, transitory underground water circulation mechanisms of discontinuous nature take place. Such water circulation phenomena are subject to seasonal cycles. This litho-stratigraphic setting comprising highly-permeable surface materials, causes infiltrations of large volumes of water in the entire area of Gimigliano. Such infiltration phenomena occur during intense rainfall events that characterize the fall and spring months over a short amount of time. This favors the rapid saturation of the covering debris materials causing high seasonal water tables. These waters, often come in the form of springs and are abundant on the left side of the landslide (coinciding with the new residential estate) [Straface *et al.*, 2012].

2.3 Pre-2010 geotechnical characterization and monitoring data

Several geotechnical investigation programs were performed since the 1990s (in 1990, 1993, 1997, 2003, 2008, 2010, 2011 and 2012), which date back to the first slope stabilization intervention attempts. Before the post-2010 investigation program, most of the geotechnical borings were drilled at relatively shallow depths (< 40 m). Thus, they were unable to characterize deeper units potentially responsible for movements of deep-seated instabilities. In this paper we focus on the investigation

program performed in 2012-2013 which the Authors followed directly. The numerous investigation programs performed over the years demonstrate the difficulty of adequately characterizing the complex Gimigliano landslide phenomenon.
Various monitoring data sources were available in the winter 2010 (after the activation of the most recent instability phenomena). Among them, we found multi-epoch satellite synthetic aperture radar (SAR) data to be particularly useful in identifying deformation fields within the town of Gimigliano. As a result, in the remainder of this section we interpret data generated by Fortunato and Ferrucci [2012] using such technique. Fig. 5 shows maps of displacement rates obtained using the Permanent scatterer (PS) interferometric SAR (PS-InSAR) technique. This technique is based on the the multi-temporal evolution in space of permanent scatterers (fixed targets in the SAR scenes such as buildings/monuments) that are used to accurately evaluate local velocity fields in the direction of an axis, called line of sight (LOS), which connects the satellite with the target permanent scatterer on the ground. Fig. 5a shows LOS velocity maps in the period 1993–2000, while Fig. 5b focuses on movements in the 2002–2010 period [from Fortunato and Ferrucci, 2012] All velocity fields shown in Fig. 5 are along the LOS. In this specific application, descending orbits were used with an Azimuth of 277° North and an angle of incidence of 23°. Thus, such velocity maps can be thought as representative of pseudo-vertical movementes since for engineering applications the angle of incidence of the satellite can be considered as sub-vertical. The SAR data used in this study were taken from the ERS-1 and ERS-2 datasets for the period 1993–2000 and from the ENVISAT dataset for the period 2002–2010. All satellites used to generate the maps shown in Fig. 5 belong to the European Space Agency.

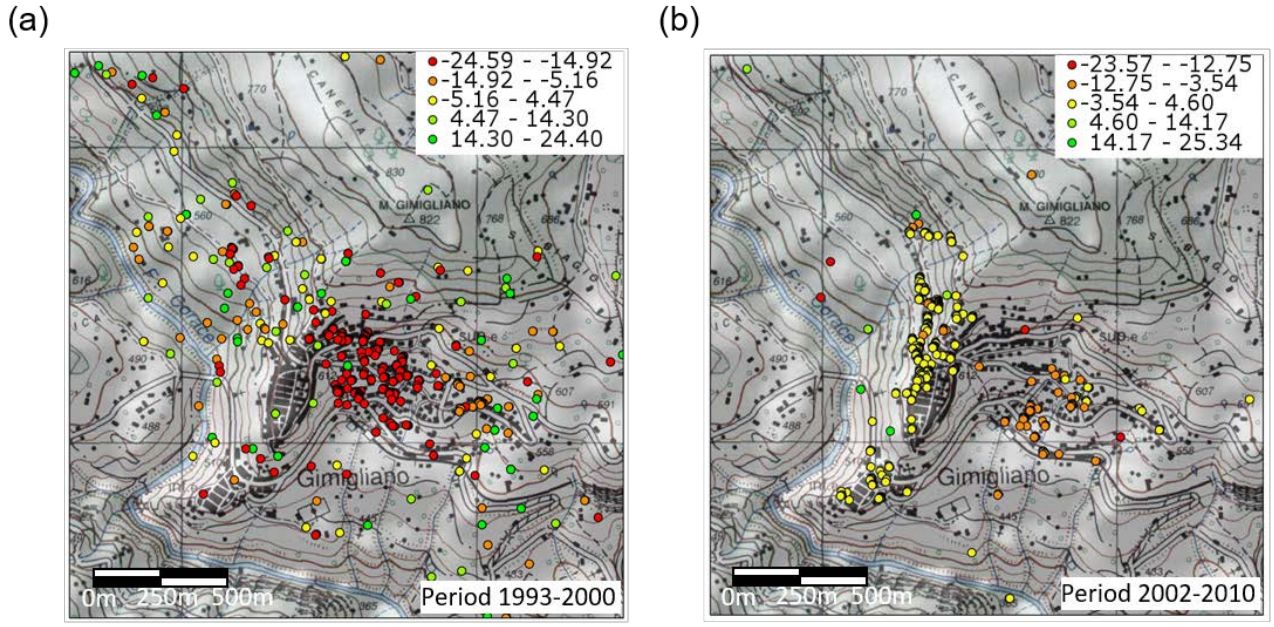

Figure 5. Map of deformation (velocities in mm/year) in the LOS direction for the following observation periods: (a) 1993-2000, and (b) 2002-2010 [adapted from Fortunato and Ferrucci, 2012].

Fig. 5a shows that in the period 1993–2000 the most significant pseudo-vertical displacements were located in the new building estate. This entire area, during this observation period showed a velocity higher than 2 cm/year (red dots). In the period 2002–2010 (Fig. 5b) the average sub-vertical deformation rates were smaller and two main areas were affected by the movement: the new building estate and the western flank of the medieval center slope. The new estate was characterized by a velocity of about 1.2 cm/year (orange dots). In this period, as shown by Fig. 5b, there seemed to be a migration of the deformation field to the western slope of the medieval center where the LOS velocity was small but not negligible witn an amplitude of about 0.3 cm/year (yellow dots).

More recent InSAR data for the periods 2010-2011 [Bianchini *et al.*, 2013] and 2014-2016 [Filomena, 2019] confirmed that the new building estate moves at a higher LOS velocity than the medieval village. Based on all analyzed datasets, it is possible to conclude that: (1) the central part of the medieval village is stable, (2) the western slopes of the medieval village are characterized by a slow rate of sub-vertical movements, and (3) the new building estate has a faster and larger sub-vertical deformation field.

2.4 Pre-2010 slope stabilization and remediation measures

Various interventions aimed at mitigating existing slope instability-related movements were carried out over the last 30 years. Two main intervention types were performed: (1) emergency and short-term repair works, and (2) measures trying to ensure medium- and long-term safety conditions. Unfortunately, as highlighted by the ongoing deformation fields still present within a large portion of Gimigliano, none of these interventions solved the problem. This is mainly due to an unsatisfactory level of knowledge of the instability phenomenon and lack of adequate financial resources. Such mitigation strategies can be broadly subdivided into three categories: (1) structural interventions, (2) drainage interventions, and (3) regimentation of surface waters and bio-engineering interventions against surface erosion. Structural interventions were mainly related to the construction of retaining walls (with and without anchors) and were performed along roads and next to structures damaged by the landslide. Drainage interventions had the purpose of lowering the water table and involved shallow (by means of drainage trenches) and deeper layers (using drainage tunnels, drainage wells, and sub-horizontal drainage pipes). The resulting drainage flow rates during rain events showed a highly variable values over time, suggesting complex mechanisms of imbibition and seepage within the superficial detrital soils.

3. Post-2010 tests program and monitoring

3.1 Field investigation data

After the paroxysmal phase of the Gimigliano landslide occurred during the winter seasons 2009-2010 a new laboratory-field test program was funded. The main goal of this investigation program was to better characterize the stratigraphic distribution of shallower units in the area of the Gimigliano landslide, identify characteristic strength values of such layers, and possibly come up with lasting mitigation strategies. In the remainder of this section main results of the field investigation program are summarized.

3.1.1 Boring logs

Most field investigation programs performed in the past 30 years included the presence of numerous borings. However, as mentioned before, none of them was deep enough to characterize deeper layers potentially responsible for deep-seated landslide-related deformations. As a result, to fill this gap, in the post-2010 field investigation program, four borings (S1-S4) were drilled at depths greater than 70 m, ranging between 70 m and 76.5 m. These borings are all located within the main body of the Gimigliano landslide (Fig. 1). S1 is located in the area of the crown of the landslide, S2 and S4 in its central portion, and S3 towards the scarp (in close proximity to the natural boundary constituted by the Corace river). All borings were equipped with piezometers, while S1-S3 were also equipped with inclinometers.

Fig. 6b, 7b, 8b, and 9 show boring logs for all four borings (S1-S4). Borings S2, S3, and S4 are approximately aligned along the A-A' section (Fig. 1). The stratigraphy of boring S1 (Fig. 6b) seems to be relatively homogeneous in terms of materials, but extremely complex in terms of degree of alteration of the various rocks layers encountered throughout the boring. Similar conclusions can be drawn looking at borings S2-S4. Interestingly, in these borings, at large depths, there are thin layers of dark, sericitic phyllites. These layers all appear to be very altered and partially argillified. Overall,

the stratigraphic succession of these borings leaves the field open to different interpretations about potential lateral continuity of the materials encountered. At various depths, the presence of the same formations but with varying thicknesses and intercalations with different sequences is found. Furthermore, some materials are present in some borings, but absent in others, as it can be seen for the ophiolites-serpentinites layer located at 27 m of depth in S2, that is not present in the other borings at any depths. Such difficulties in interpreting the lateral continuity of stratigraphic layers is partially due to the presence of various instability phenomena at various depths and involving different volumes, and partially related to the extremely complex active tectonic of the area that involves the presence of fault segments and splays, alternated with tectonic foldings. Overall, based on the geological/tectonic background of the area and the stratigraphies of borings S1-S4, it is possible to recognize the following layer successions within the Gimigliano landslide: an ophyolitic unit overlying a serpentinites/metabasities layer of variable thickness that is, in turn, covering a thin phylladic layer on top of a deeper unit of intact phylladic schists (predominantly grey) with intercalations of levels of quartz.

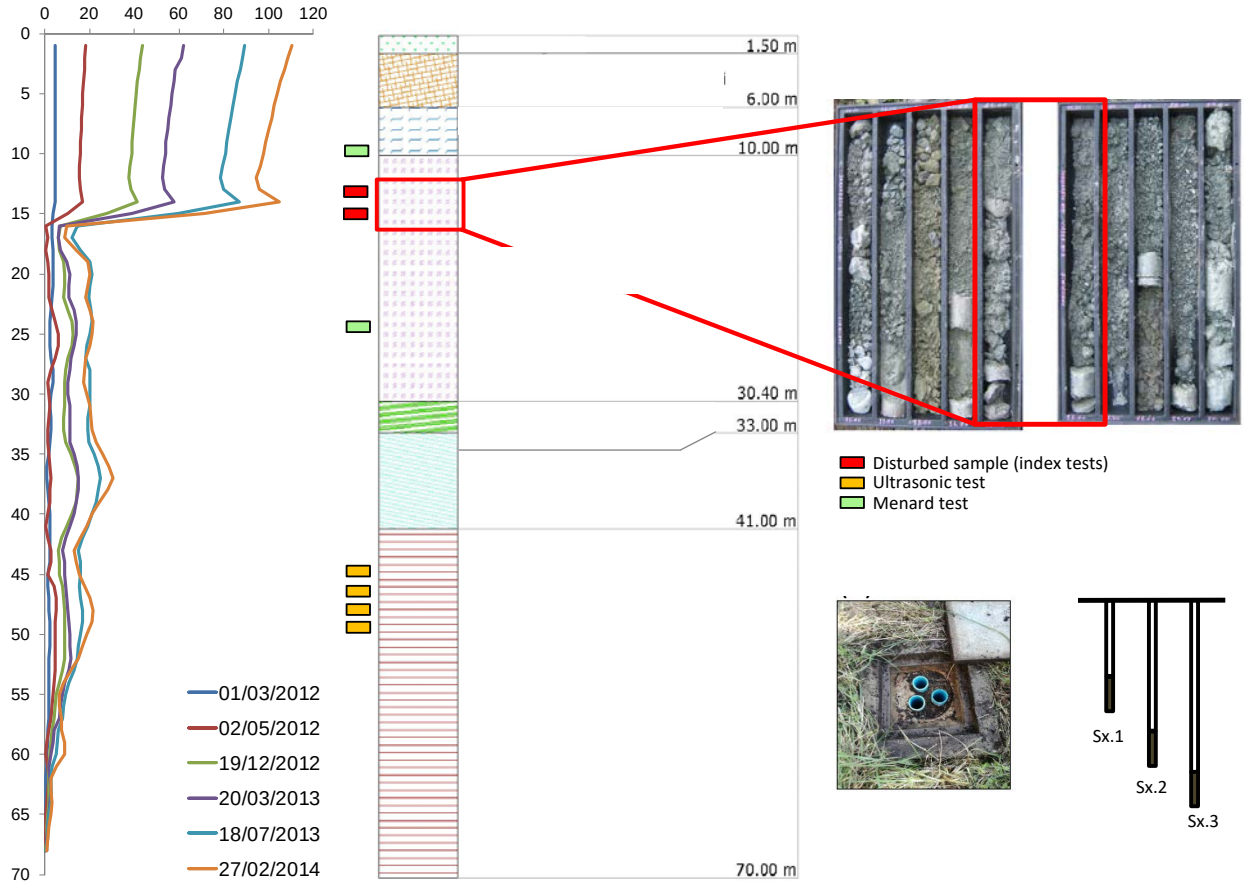

Figure 6. (a) inclinometer data during the period 2012-2014, (b) boring log, and (c) photo of disturbed samples collected in the area corresponding to the highest cumulative inclinometer displacement for boring S1, (d) sample photo of the spatial distribution of the piezometers, and (e) schematic showing th cross section of the installed piezometers.

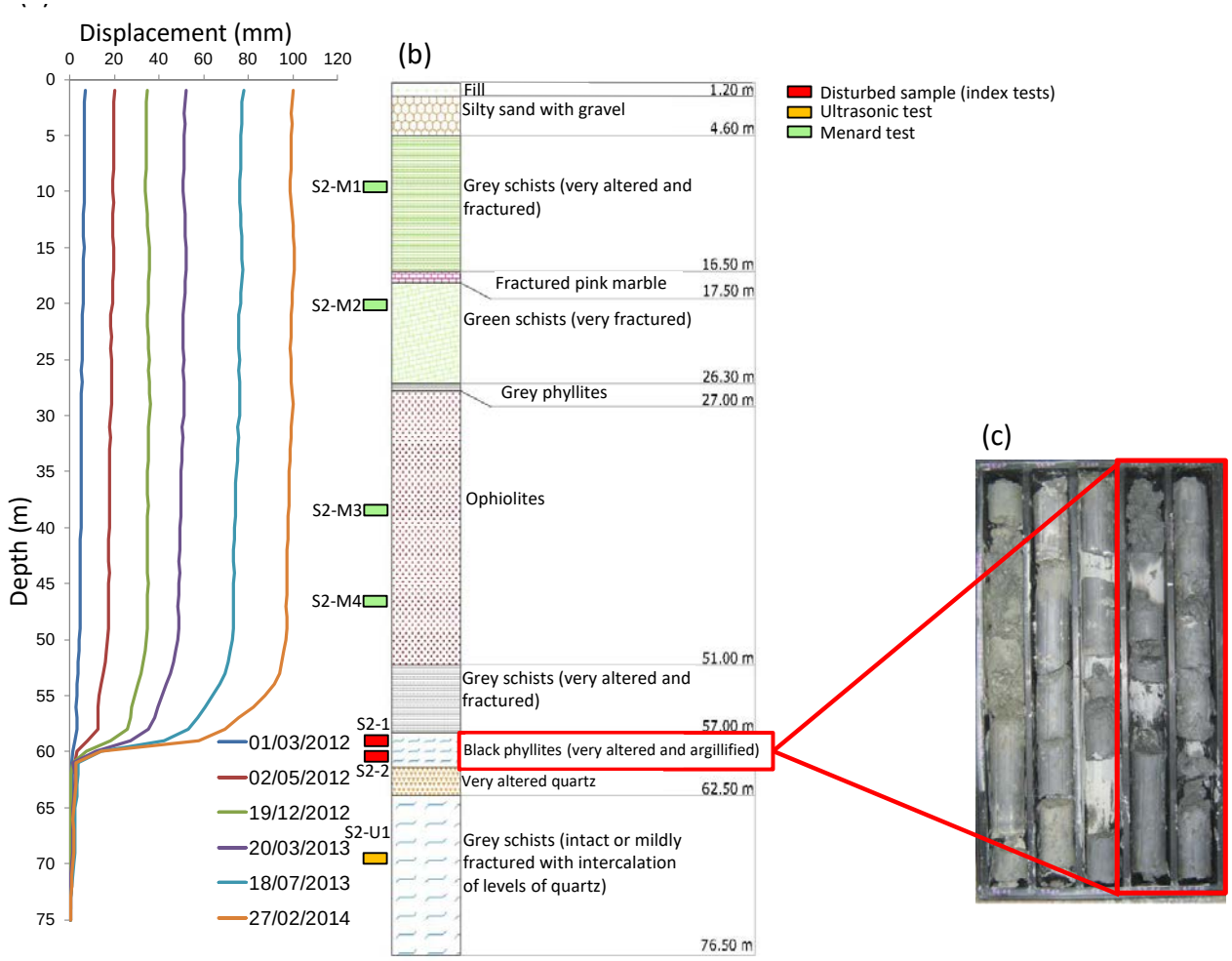

Figure 7. (a) inclinometer data during the period 2012-2014, (b) boring log, and (c) photo of disturbed samples collected in the area corresponding to the highest cumulative inclinometer displacement for boring S2.

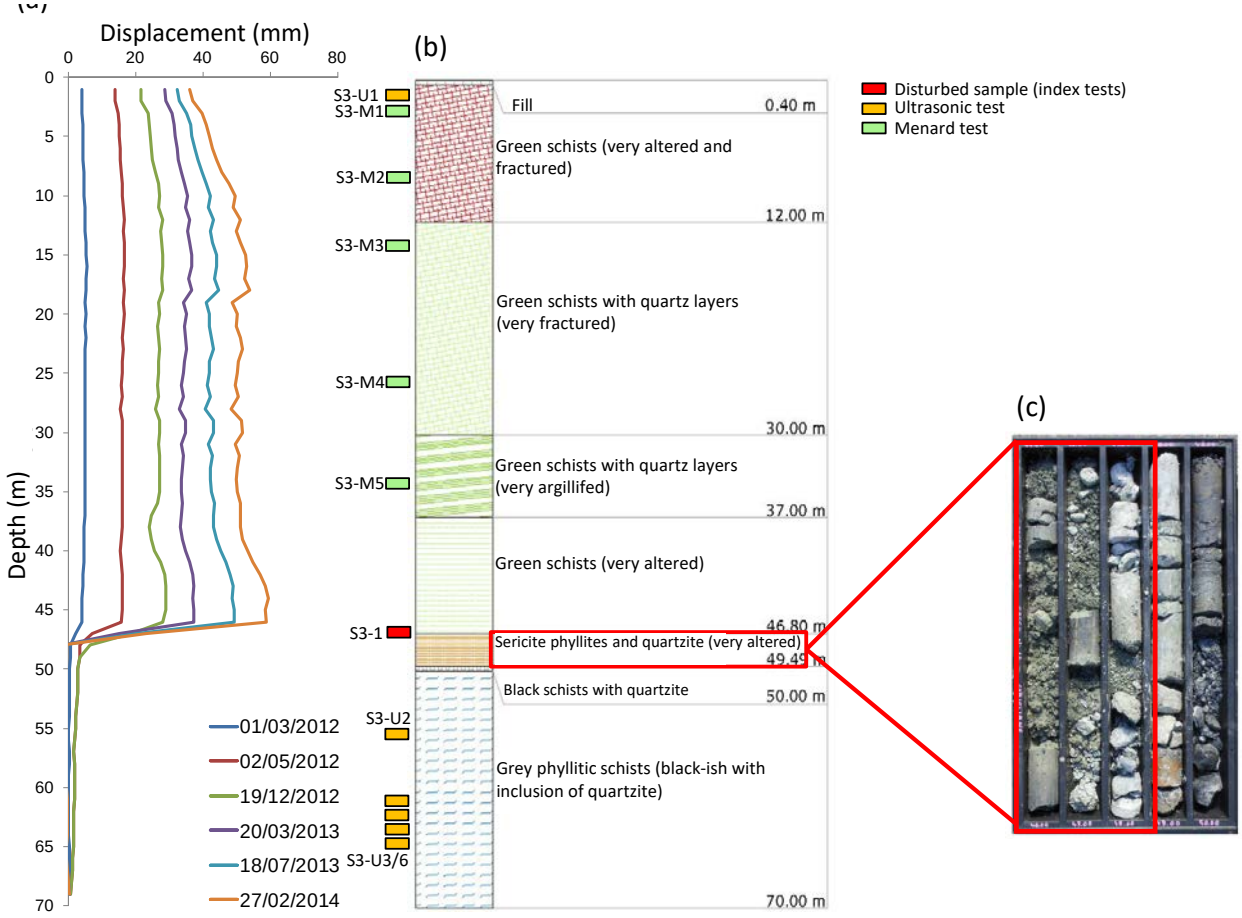

Figure 8. (a) inclinometer data during the period 2012-2014, (b) boring log, and (c) photo of disturbed samples collected in the area corresponding to the highest cumulative inclinometer displacement for boring S3.

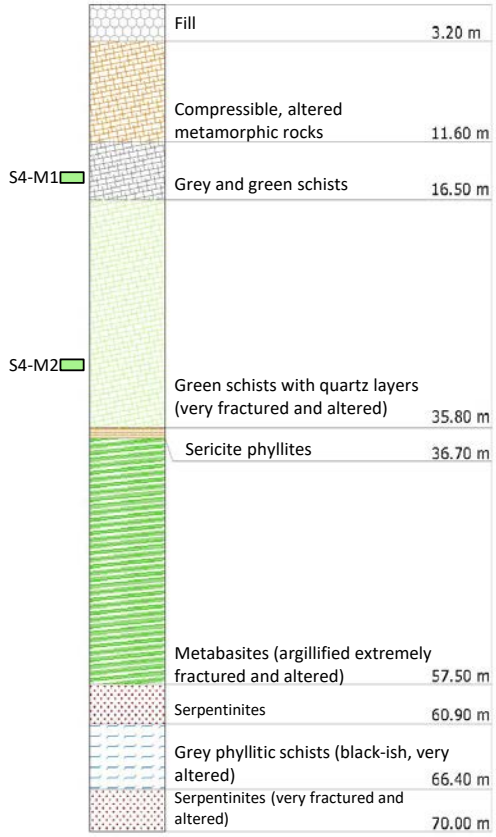

Figure 9. Boring log and stratigraphic description of S4.

3.1.2 Slug tests

Slug tests are a useful and relatively inexpensive tool to characterize the hydraulic conductivity of rock masses and soils. They are typically performed within open groundwater wells, where water is added (or removed), and the change in hydraulic head is monitored over time. In order to estimate the value of the hydraulic conductivity of the rock mass involved in the Gimigliano landslide, several slug tests were performed within the piezometers located in borings S1-S3. The hydraulic conductivity values obtained by means of the slug tests are summarized in Table 1. Measured hydraulic conductivity values range between 1E-05 to 5E-06 m/s and are generally in agreement with values expected for fractured rocks.

Table 1. Slug test results in borings S1-S3.

Boring	Depth range	Slug test results	
		Layer description	**Hydraulic conductivity**
	m	-	m/s
S1	3.0 - 18.0	Green schists (very altered)	N.D. (dry)
S1	33.0 - 39.0	Green schists (very altered)	N.D. (dry)
S1	3.0 - 50.0	Green schists (intact to altered)	N.D. (dry)
S2	6.0 - 13.0	Grey schists (very altered)	1.56E-05
S2	16.0 - 25.0	Grey schists (very altered)	2.17E-05
S2	30.0 - 40.0	Ophiolities-Serpentinites (very alterd)	1.19E-05
S3	2.0 - 8.0	Green schists (very altered)	N.D. (dry)
S3	14.0 - 30.0	Green schists with quartz intercalations	2.98E-05
S3	38.0 - 47.0	Green schists (altered)	5.48E-06

3.1.3 Pressuremeter tests

Ten Menard-type pre-bored pressuremeter tests were performed to better define the mechanical properties of the rocks. The locations at which these tests were performed are shown in Fig. 6b-8b and 9. Fig. 10 shows pressuremeter test results at borings S1-S4 in terms of pressuremeter limit pressure (P_L), elastic modulus (E_M), and E_M/P_L ratio. These test results show a large variability of all reported parameters. Such strong variability is evident in different units, but it is also evident within the same layer and has to do with the strong variability of the degree of alteration and weathering of the materials being analyzed [Ausilio and Zimmaro, 2014]. This almost chaotic distribution of the pressuremeter parameters, along the whole depth of the borings, is a quantitative confirmation of the extremely complex and variable stratigraphy involved in the Gimigliano landslide instability phenomenon. Such complexity was already observed in the boring logs shown in Fig. 6b-8b and 9.

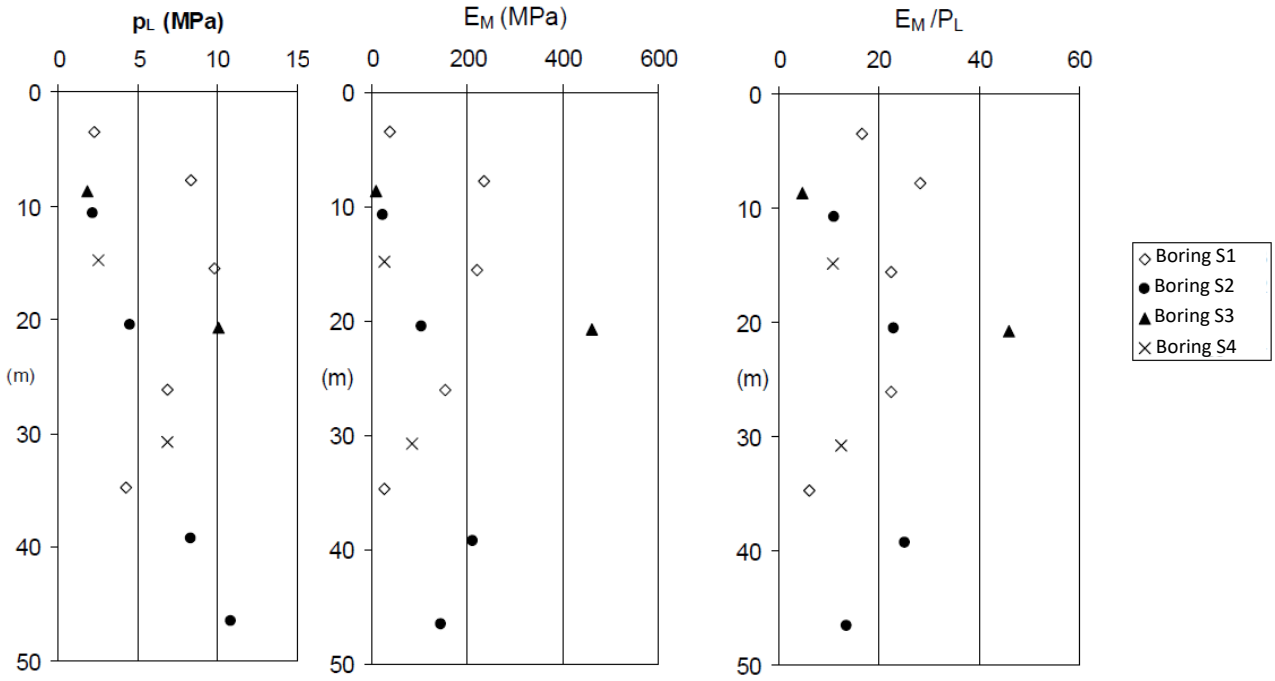

Figure 10. Pre-bored pressuremeter test results.

3.1.4 Electrical resistivity tomography

The electrical resistivity tomography (ERT) is a widely-used non-invasive geoelectrical method that can be used to reconstruct the geometry of shallow geological structures. Such reconstruction is performed utilizing the electrical resistivity of geo-materials, which in turn, is related to their physical properties and/or states. As a result, this non-invasive method can be a useful tool for investigating landslide areas, identify geologic units involved, and possibly identify the degree of lateral continuity between units. For investigating the Gimigliano landslide area, seven ERT high resolution surveys (one longitudinal and six transversal to the landslide body) were performed (Fig. 11). These surveys have a length range between 235-940 m and investigation depths between 35 m and 140 m. Additional technical details on these tests are provided by Ausilio and Zimmaro [2017]. The ensemble analysis of the tomographies shown in Fig. 11, highlights a chaotic distribution of the resistivity values with high variations in both directions (horizontal and vertical). In some profiles, the resistivity values vary in the range 5-900 Ohm·m (Fig. 11).

Fig. 12 shows the longitudinal profile (T4), which is almost parallel to the main landslide. In the shallow portion of the profile, towards the scarp of the landslide (in the vicinity of the Corace river) and for a length of ~500 m (roughly going from x = 500 m and x = 940 m) it is possible to identify a layer with high resistivity values (> 800 Ohm·m; marked as E1 in Fig. 12). In the central portion of the profile, at depths > 35 m below the surface, there are two areas (E2) with low resistivity values (< 100 Ohm·m). These low-resistivity zones are separated by a sub-vertical discontinuity characterized by high resistivity values. In the upper part of the profile (towards the north end of the new building estate, immediately below the landslide crown area) there is a zone (E3) characterized by with medium-to-low resistivity values (< 300 Ohm·m). In the same area, at depths > 30 m below the surface there is a zone with medium-to-high resistivity values (> 500 Ohm·m). This deeper zone is separated by two sub-vertical discontinuities by two adjacent zones characterized by low resistivity values. Lastly, at the beginning of the upper zone of the profile there is another zone (E5) with medium-to-high resistivity values (> 450 Ohm·m). Overall, the profile clearly shows weakness planes and discontinuities with very low values of resistivity. Such discontinuities can be identified where the gradient of resistivity changes rapidly. Sub-horizontal discontinuities may be related to weakness planes and can be associated with translational and/or rotational deformation phenomena. On the other hand, sub-vertical discontinuities are related to tectonic structures such as primary faults and/or secondary splays/segments. ERT-related information will be analyzed, in a subsequent section, together with boring log and monitoring data, to obtain a final reconstruction of the instability phenomenon.

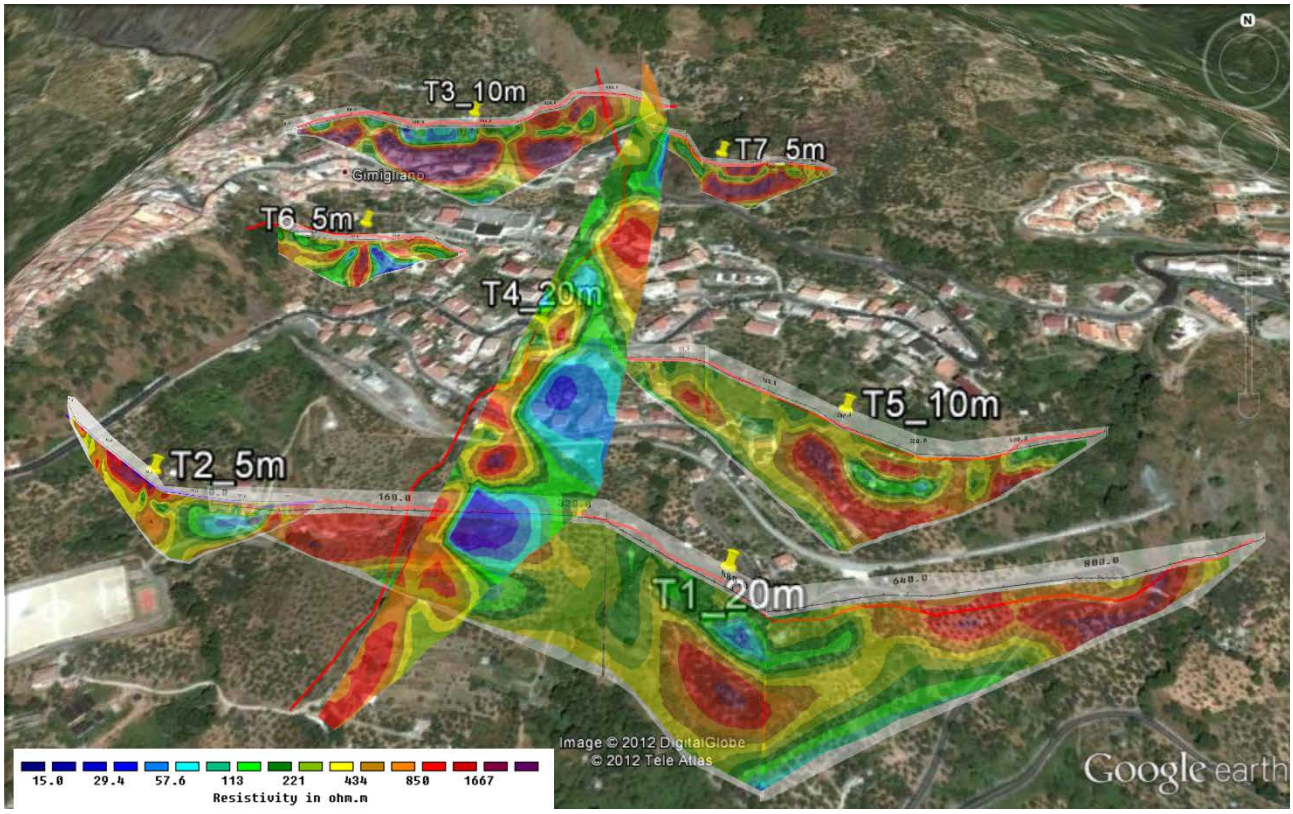

Figure 11. Traces of the electrical resistivity tomographies performed in the Gimigliano area [adapted from Rizzo *et al.*, 2012].

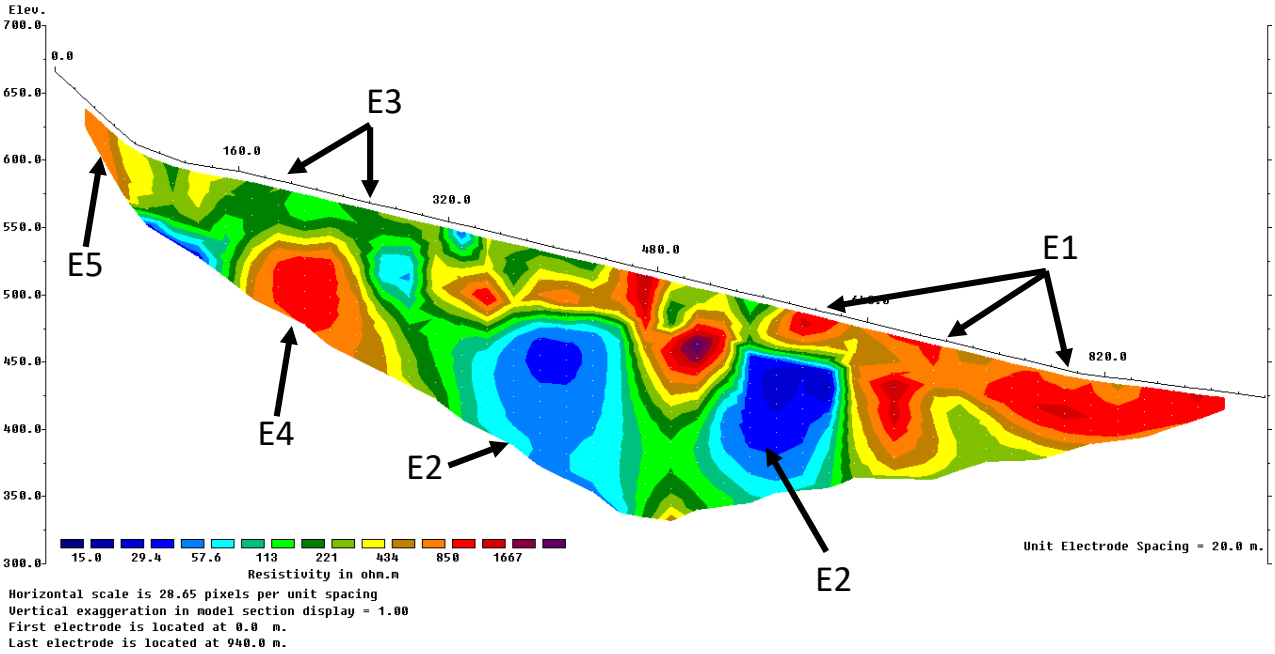

Figure 12. Resistivity values measured along the N-S section roughly coincident with section A-A' shown in Fig. 1 [adapted from Rizzo *et al.*, 2012].

3.2 Landslide monitoring

3.2.1 Piezometer data

A careful interpretation of the pore pressure field is important to assesspresent slope stability conditions and their potential changes. This is a key problem when dealing with structurally complex formations. For this purpose, three open standpipe piezometers were installed in borings S1-S3 in 2012 (Fig. 6d,e). Table 2 reports their depths and identification names. All piezometers in S1 were installed in grey schist layers with variable degree of alterations. The deeper piezometer installed in S2 is located within a thick ophiolitic layer, while two shallower piezometers were installed within the grey and green schist layers, respectively. Similarly, the two shallower piezometers installed in S3 are located within green schist layers, while the shallower piezometer installed within this boring is located in the sericitic phyllities layer at a depth equal to 47 m below the surface.

Table 2. Piezometer depths and identification names.

Boring	Piezometer name	Piezometer depth (m)
S1	S1.1	18
S1	S1.2	39
S1	S1.3	50
S2	S2.1	13
S2	S2.2	25
S2	S2.3	42
S3	S3.1	8
S3	S3.2	30
S3	S3.3	47

Piezometer data were recorded between 2012 and 2019. All available piezometer readings are summarized in Table 3. The remainder of this section includes some interpretation about the complex distribution of hydraulic heads/piezometric surfaces in the area. However, such interpretation is limited to data collected at three individual points (thus, rigorously, to one-dimensional profiles) that cannot capture all nuances of such complex, strongly three-dimensional, underground phenomena. At the S1 location, the water table has always been deeper than all piezometers (> 50 m below the surface). The water table measured within S2 was located ~8 m below the surface in 2012, while in the period 2018-2019 was located at deeper depths (~15 m below the surface). The water table reconstruction at S3 is more complicated. On average, piezometer readings were around ~20 m below the surface. However, some differences have been observed between the piezometers located in the green schist layers and that located within the sericitic phyllites layers. Such differences may be related to the different pore pressure equalization times and response lags that these two units may present due to different hydraulic conductivity values. Such conclusion is confirmed by slug test data presented in Section 3.1.2 (*i.e.*, the sericitic phyllites layer is less permeable, by an order of magnitude, than the green schist layers). As a whole, this body of measurements, do not provide a robust hydrogeological characterization to use in forward or back-analysis of the instability phenomenon. This is mainly due to the complexity of the structural-geological setting and the presence of several water springs and drainage interventions such as drainage tunnels and trenches (described in Section 2.4).

Table 3. Piezometer reading in the period 2012-2019.

Date	Piezometer Reading (m)								
	S1.1	S1.2	S1.3	S2.1	S2.2	S2.3	S3.1	S3.2	S3.3
12-Jun-12	Dry	Dry	Dry	8.75	8.75	8.75	Dry	20.30	33.60
20-Dec-12	Dry	Dry	Dry	8.46	8.46	8.46	Dry	21.47	33.47
25-Oct-18	Dry	Dry	Dry	Dry	15.25	15.25	Dry	20.45	22.00
31-Oct-18	Dry	Dry	Dry	Dry	15.20	15.20	Dry	20.10	21.65
02-Nov-18	Dry	Dry	Dry	Dry	15.10	15.10	Dry	19.84	21.50
07-Dec-18	Dry	Dry	Dry	Dry	15.30	15.30	Dry	19.08	20.92
27-Dec-18	Dry	Dry	Dry	Dry	15.27	15.27	Dry	18.90	20.70
04-Jan-19	Dry	Dry	Dry	Dry	15.37	15.37	Dry	18.93	20.80
04-Sep-19	Dry	Dry	Dry	Dry	Dry	36.40	Dry	22.40	23.80

3.2.2 Inclinometer measurements

When dealing with ongoing landslide-related deformation phenomena, inclinometer data may constitute an extremely useful piece of information. A total of three inclinometers were installed in borings S1-S3 to monitor horizontal displacementsagainst depth. Inclinometer measurements were performed in the period 2012–2014 (Fig. 6a, 7a, and 8a). Measurements within boring S1 show displacements located at a relatively shallow depth (15-16 m below the surface). This movement may be related to shallower instability mechanisms taking place within the covering debris materials. This instability mechanism is unlikely related to the large Gimigliano landslide, but it is more likely a more local mechanism. Measurements performed within S2 and S3 (roughly aligned along section A-A' presented in Fig. 1) show that at these locations, relative movements occur at a depth of 58–60 m and 46–48 m, respectively. The cumulative displacements observed within borings S2 and S3 are localized within a narrow band that corresponds to the location of a very altered black sericitic phyllites layer. Therefore, it is possible to conclude that a clear and narrow shear band occurs within this thin layer. Fig. 7c and 8c show photos of the material sampled within this layer. Index tests and

particle size distribution analyses were performed on these materials. Results from these laboratory tests are presented in Section 3.3.1. Measurements within borings S2 and S3 allowed us to identify a deep-seated movements occurring within the thin phyllites layer. By looking at these inclinometer data, it is possible to argue that this deeper instability phenomenon is what causes the Gimigliano landslide that affects a large portion of the new building estate.

3.2.3 Structural damage monitoring

As indicated in the Introduction, an analysis of damage affecting structures and infrastructure systems can yield very useful kinematic information on active landslides. For the Gimigliano landslide, such opportunity is offered by data collected by the local branch of the Italian Department of Civil Protection (DCP) after the re-activation of the Gimigliano landslide in 2010. They established a temporary office to monitor cracks occurring throughout the town to civil structures and infrastructure systems such as buildings, retaining structures, roadways, bridges, buildings, and railroad tracks. (Fig. 13). Such damage assessment was performed in a rather qualitative manner and crack widths were not consistnely recorded. The main goal of this damage monitoring effort coordinated by the Italian DCP was to identify priority areas for local interventions to mitigate infrastructural collapse risk. However, in this paper, rather than using this data to analyze the severity of structural and infrastructural damage per se, we utilize this information to identify key kinematic features of the landslide. As a result, this data constitutes a useful piece of information to understand the rate of movements and distinuguish stable areas from more active zones. The inspections were performed in the periods 2013-2014 and 2015-2018. A total of 54 structures, located in various zons of the unstable area were monitored. Each of them received a unique identification number (ID).Fig. 14 shows the evolution of a representative building (ID #46) where cracks at a column-beam joint of a reinforced-concrete building were monitored in the period 2013-2018. This building is located next to boring S3 (instrumented with an inclinometer, Fig. 8). We combined this information with pre- and post-2010 InSAR deformation maps (providing information on shallow sub-vertical movements) and inclinometer data (related to deep horizontal movements) to characterize the temporal and spatial evolution of the Gimigliano landslide. This approach allowed us to have a complete monitoring system by combining and enhancing information from novel (*i.e.*, the InSAR data) and traditional (*i.e.*, the structural damage evolution in time) techniques.

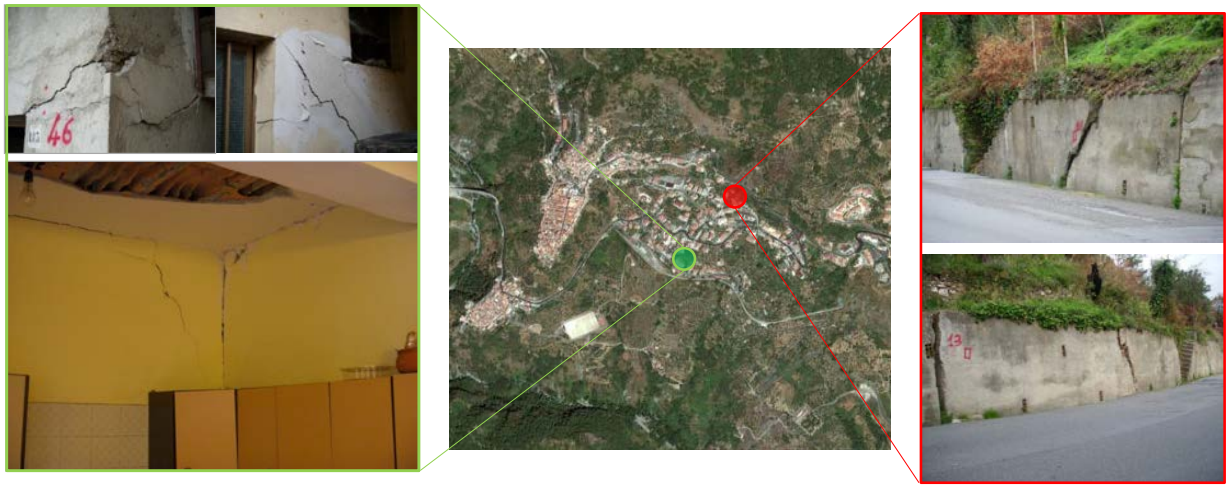

Figure 13. Sample photos of landslide-induced damage within the new building estate area of Gimigliano.

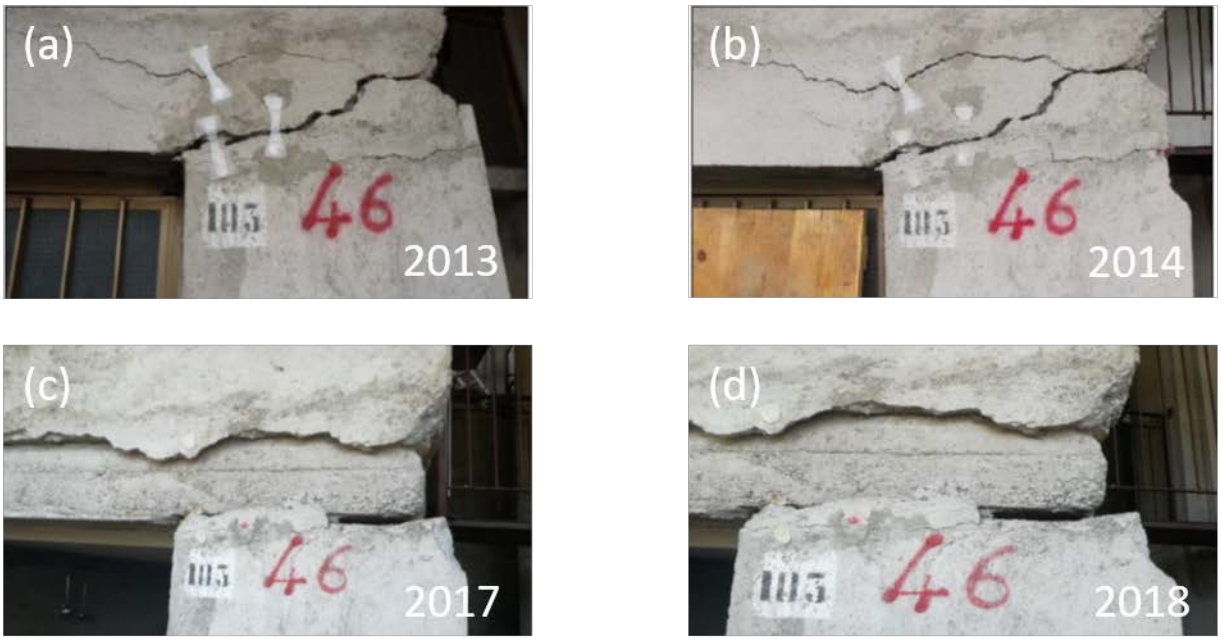

Figure 14. Photos of a crack at a column-beam joint monitored in the period 2013-2018 for structure #46, next to boring S3: (a) 2013, (b) 2014, (c) 2017, and (d) 2018.

3.3 Laboratory tests

3.3.1 Particle size distribution and index tests

Index tests and grain size distribution analyses were performed on disturbed samples collected at borings S1-S3. The location of these samples are shown in Fig. 6b, 7b, and 8b. Samples within boring S1 were collected in the green schist layers. Within these layers, typical soil types are silty gravels with sands. The fines content of these materials ranges between 7-25%. Samples collected in borings S2 and S3 are from the thin sericitic phyllites layer where the shear zone responsible for the Gimigliano landslide is located. It is very altered and argillified material and comprises silty sands with gravels and silty gravels with sands. The range of fines content in this layer is 13-18%. Table 4 summarizes results of the grain size distributions observed in these samples. The granulometric distribution for samples collected in borings S2 and S3 are shown in Fig. 15.
Table 5 reports Atterberg limits from tests performed on the fines portions of the same disturbed samples summarized in Table 4. They show a plasticity index in samples collected in boring S1 ranging between 6% and 11.5%. The plasticity index in the sericitic phyllites from borings S2 and S3 ranges between 8.5% and 16%. Fig. 16 shows the Casagrande chart for the fines portion of samples collected in borings S1-S3. All samples are classified as low plasticity clays.

Table 4. Grain size distribution of samples collected in borings S1-S3.

Boring	Depth range	Grain size distribution			
		Description	Silt	Clay	FC
	m	-	%	%	%
S1	14.8 - 15.0	Silty Gravel with Sand slightly clayey	20	5	25
S1	16.0 - 16.2	Gravel with Sand slightly silty	6	1	7
S2	58.0 - 58.3	Silty Sand with Gravel slightly clayey	13	5	18
S2	59.0 - 59.2	Silty Sand with Gravel	9	4	13
S3	46.4 - 46.6	Silty Gravel with Sand	15	3	18

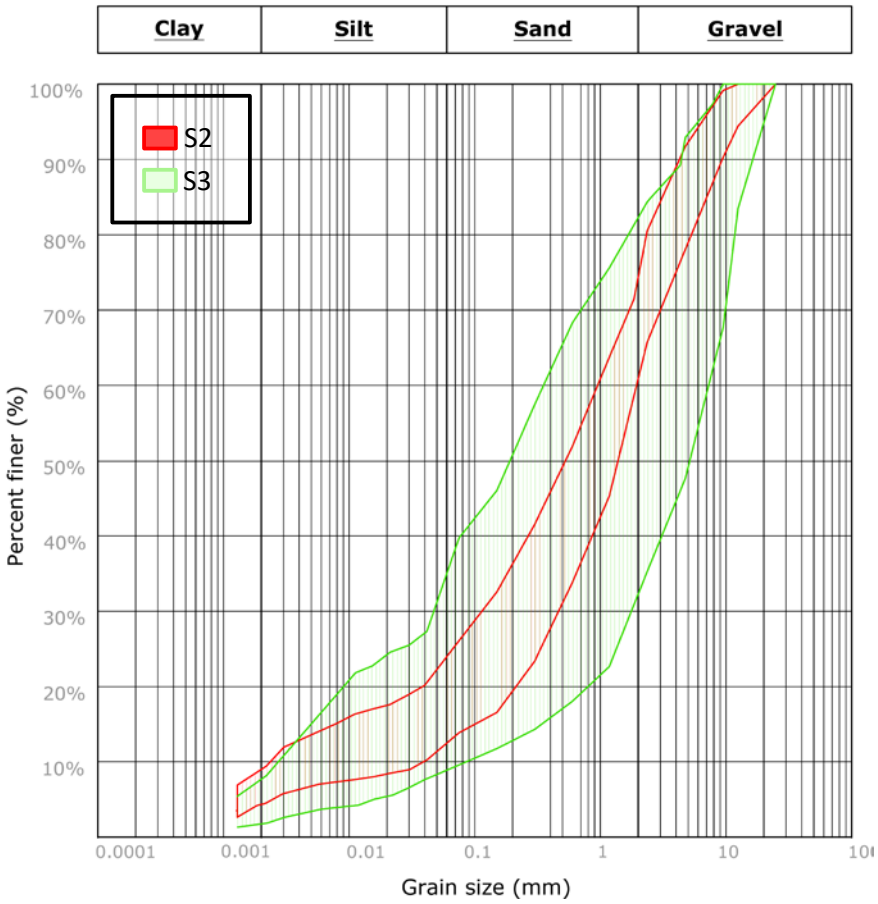

Figure 15. Grain size distribution ranges of samples collected in borings S2 and S3.

Table 5. Atterberg limits of samples collected in borings S1-S3.

Boring	Stratigraphic description		Atterberg limits		
	Depth range	**Layer**	**W_L**	**W_P**	**PI**
	m	-	%	%	%
S1	14.8 - 15.0	Green schists (very altered, argillified)	21	15	6
S1	16.0 - 16.2	Green schists (very altered, argillified)	26	14.5	11.5
S2	58.0 - 58.3	Black phyllites (very altered, argillified)	29	17	12
S2	59.0 - 59.2	Black phyllites (very altered, argillified)	33	17	16
S3	46.4 - 46.6	Sericite phyllites and quartzite (very altered)	22	13.5	8.5

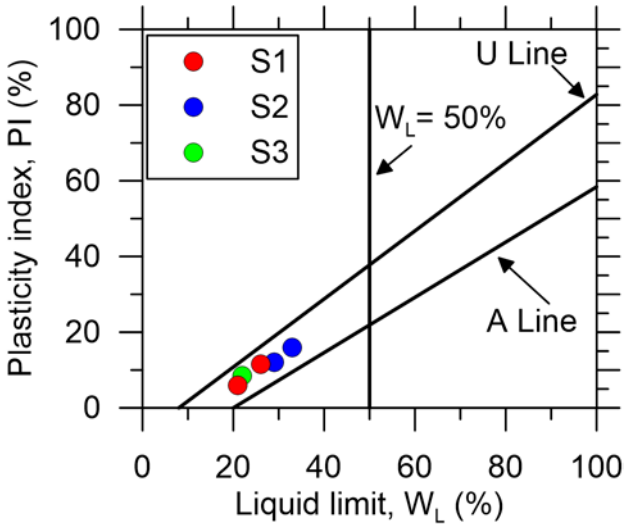

Figure 16. Casagrande chart of the fines portion of samples collected in borings S2 and S3.

3.3.2 Ultrasonic testing for the determination of P- and S-wave velocity

In order to better characterize the rock masses involved in the complex Gimigliano landslide, several rock samples were collected in borings S1-S3. For each of them we determined P and S wave velocity values (V_P and V_S) by means of ultrasonic laboratory testing. The locations of these samples are shown in Fig. 6b, 7b, and 8b. Various rock types are present in the area. In addition to this between-rock type variability, within the same rock type, the degree of alteration and weathering is also extremely variable. Such strong between- and within-rock variability makes the characterization of the materials involved in the Gimigliano landslide particularly challenging as it has been observed analyzing pre-bored pressuremeter tests (Section 3.1.3).

The Ultrasonic testing procedure is a simple and non-destructive test type that is being increasingly used in geotechnical applications. The velocity of ultrasonic waves in rocks is commonly used as an index in evaluating microstructure and associated properties of rocks [Basu and Aydin, 2006]. A number of investigators [Gaviglio 1989; Kahraman, 2001; Ozkahraman *et al.*, 2004; Yasar and Erdogan, 2004; Kahraman *et al.*, 2005; Sharma and Singh, 2008; Kahraman and Yeken, 2008] recently studied the relationship between different physical (*e.g.*, density, porosity, void ratio, and absorption by weight) and mechanical (*e.g.*, uniaxial compressive strength, tensile strength, modulus of elasticity, and shear strength) properties of rocks and V_P, concluding that V_P is closely related to these properties. Such strong correlations make it attractive to use V_P values of rocks as proxies for various physical-mechanical properties of such materials.

In this study, V_P and V_S of rock specimens are determined using a Portable Ultrasonic Non-destructive Digital Indicating Tester (PUNDIT) in accordance with ASTM D2845 standards (ASTM, 2008). The PUNDIT testing machine used in this study has a pulse transmission generator, two transducers, and an electronic counter (tester) for time interval measurements. The transducers (with diameter of 50 mm and frequency of 54 kHz) consist of a transmitter that converts electrical pulses into mechanical pulses and a receiver that converts mechanical pulses into electrical pulses. The transmitter–receiver transducer pairs are placed on two opposite faces of the rock sample (Fig. 17). The rock surfaces are polished to a sufficiently smooth plane and covered with a thin film of stiff grease to provide good coupling. V_P and V_S values are calculated from the measured travel time and the distance between the two transducers (transmitter and receiver). The measured time is the sum of the real time through the rock sample and the time delay due to transducers lag. This time delay is determined by adopting a face-to-face method as recommended in the ASTM D2845 (ASTM, 2008)

standards. Such method consists in placing the transducers in direct contact with each other and measuring the delay time directly.

In this study, we selected only specimens with a length greater than 10 cm and smaller than 18 cm. Such length range has been adopted out of practicality. We found that shorter specimens may have problems in the stability of the measurement due to the stronger influence of the transducers delay for short paths. Longer specimens were just unpractical to use. All specimens have a diameter equal to 8.4 cm. Fig. 18 shows all specimes used in this study. On each rock sample, the V_P and V_S measurements were conducted several times with two separate transducers (shown in Fig. 16a and 16b) to test the accuracy of the measured velocities. The average value of ultrasonic pulse velocity measurement results obtained from the two instruments was then calculated and used. Table 6 reports a summary of V_P, $V_S$and V_P/V_S ratios calculated for all specimens. The analysis of Fig. 18 and Table 6 highlights an extreme variability of V_P values across the analyzed specimens. This is in part due to the fact that we tested various geologic units. Furthermore, all analyzed specimens have visible within-sepcimen horizontal and/or vertical variability due to the presence of intercalations, micro-cracks, traces of brittle and ductile tectonic deformations, and other heterogeneity indicators. Such characteristics have a strong influence on the measurements we performed and generated the high degree of V_P values variability we observed. We unsuccessfully attempted to correlate V_P values with electrical resistivity values measured within the same layers. We argue that this lack of correlation is due to the extremely variable, almost chaotic nature of these rock units and to the different measurement scales of these two investigation types.

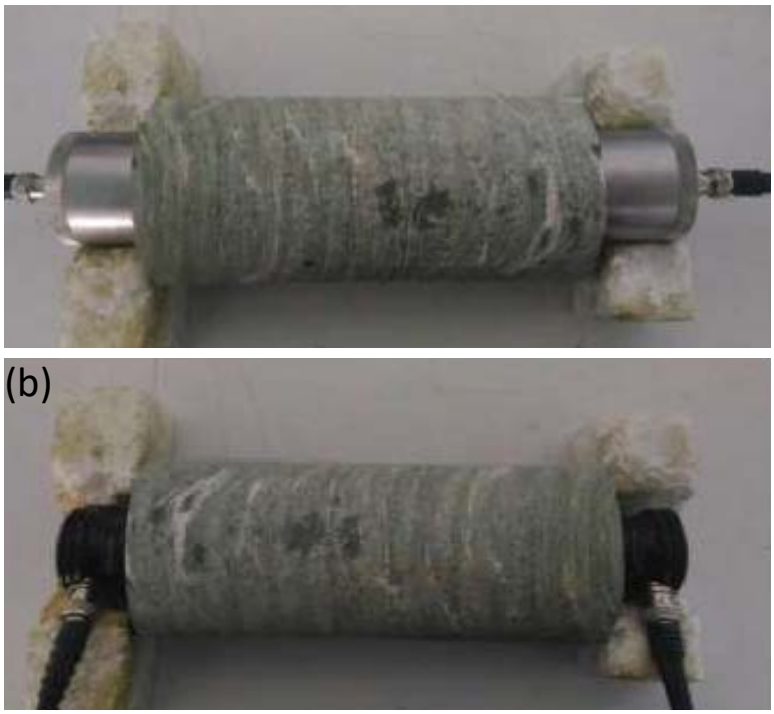

Figure 17. Two PUNDIT Transmitter–receiver transducer pairs set ups used in this study, (a) for V_P and (b) for V_S.

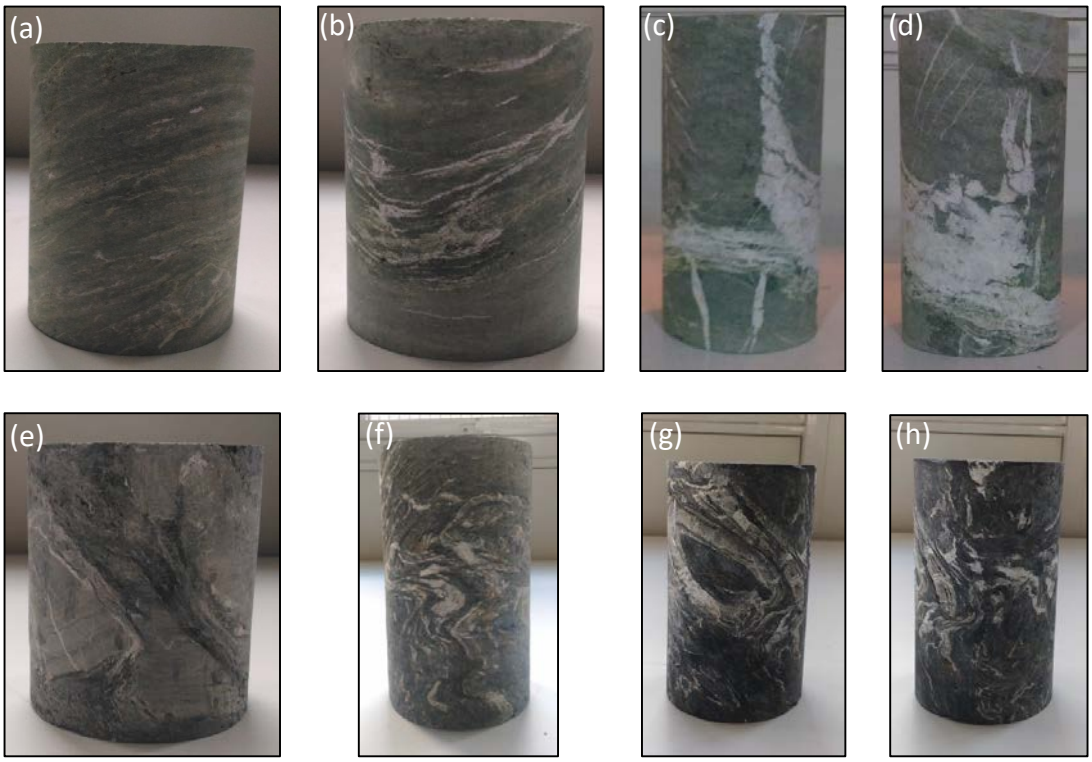

Figure 18. Specimes tested using the ultrasonic testing method for the determination of V_P values: (a) S1-45, (b) S1-46, (c) and (d) S1-48, (e) S2-68.70, (f) S3-56, (g) and (h) S3-63(1).

Table 6. Summary of V_P, V_S, and V_P/V_S values obtained by means of the ultrasonic testing method.

Specimen ID (boring-depth, m)	V_P (m/s)	V_S (m/s)	V_P/V_S
S1-44.80	5916	3127	1.89
S1-45	5150	3280	1.65
S1-46	5888	3735	1.80
S1-48	5781	3339	1.55
S1-49	4714	2825	1.41
S2-68.80	3266	1372	1.16
S3-1.80	4454	2474	3.25
S3-56	1810	506	3.58
S3-62.50	2358	1142	2.06
S3-63	3118	1541	2.02
S3-63(1)	3466	1466	2.36
S3-63.70	1825	907	2.01

4. Discussion and Conclusion

Landslide events are complex geological, geomorphological, hydrogeological, hydrological, and mechanical processes caused, exacerbated, and/or re-activated by a variety of factors. Therefore, it is very difficult to classify existing phenomena and predict their future occurrences and dynamics. In this study we apply a combined laboratory-field testing-monitoring program to characterize the complex Gimigliano landslide. The area is characterized by large-scale ground deformations due to tectonic phenomena and falls within a complex and constantly evolving geomorphological context. We utilize traditional and innovative techniques to identify responsible factors for the periodic re-

activation of this phenomenon, defining the volumes involved in the landslide and the units responsible for the complex movements occurring within a deep and very thin shear band formed within a sericitic phyllites unit. The basic stratigraphic layering hypothesized a-priori as a working assumption and based on geological analyses has been confirmed by invasive geotechnical field investigation results (*i.e.,* boring logs and pre-bored pressuremeter tests) and non-invasive geophysical tests (*i.e.*, electrical resistivity tomographies). Such stratigraphy involves a shallower cover of debris materials overlying the materials of the Frido Unit that includes metamorphic ophiolitic rocks and philladic schists. Interferometric SAR data allowed us to identify the area of the town of Gimigliano interested by landslide-related movements (*i.e.,* the new building estate) and their evlution in time. Such data also allowed us to discern between active deformation areas and stable zones (*i.e.,* the medieval village). The combination of multi-epoch SAR data and structural damage assessment information allowed us to correctly define the effects of landslide-related movements on the built environment. Such information is particularly useful for civil protection plan and emergency response efforts. Inclinometer measurements were used to identify shallower movements towards the crown of the landslide as well as the location of a thin shear band, localized within the sericitic phyllites layer present in borings S2, S3, and S4, responsible for the deep-seated Gimigliano landslide. Utilizing SAR, inclinometer, and structural damage data we reconstructed the evolution of this instability phenomenon in time during a decade-long period. Such piece of information, obtained combining these three datasets, is particularly useful as taken individually each of them would have had temporal gaps.

Three open standpipe piezometers were installed in borings S1-S3 to identify key characteristics of underground water circulation phenomena. These measurements were not sufficient to obtain a robust hydrogeological characterization, because of the complexity of the structural-geological setting and the presence of several drainage tunnels and trenches. Slug tests were used to determine the hydraulic conductivity of rock masses involved in the landslide. Laboratory test results confirmed that the analyzed rock masses are characterized by a pronounced horizontal and vertical between and within-rock type variability.

The combination of all of the above data and measurements led us to construct a final model of the Gimigliano landslide and draw the most likely failure surface on the A-A’ cross section shown in Fig. 1. This final model, presented in Fig. 19, superimposes S2 and S3 stratigraphies and a roughly co-located electrical resistivity tomography profile. This final model is the end result of years of analysis of existing historical data, damage assessments, field investigation and monitoring results, and laboratory test data. It can be effectively used for future mitigation strategies and civil protection purposes.

The characterization of the Gimigliano landslide case study that we illustrated in this study highlights the potential and the need for integrating multi-source data and measurements to analyze complex instability phenomena. Through the lens of this case study we tried to show how to combine different pieces of information from various tools and techniques, highlighting pros and cons of each of them. Such combined-technique approach may be used in the future to manage new and ongoing instability phenomena and effectively design temporal or long-term mitigation strategies.

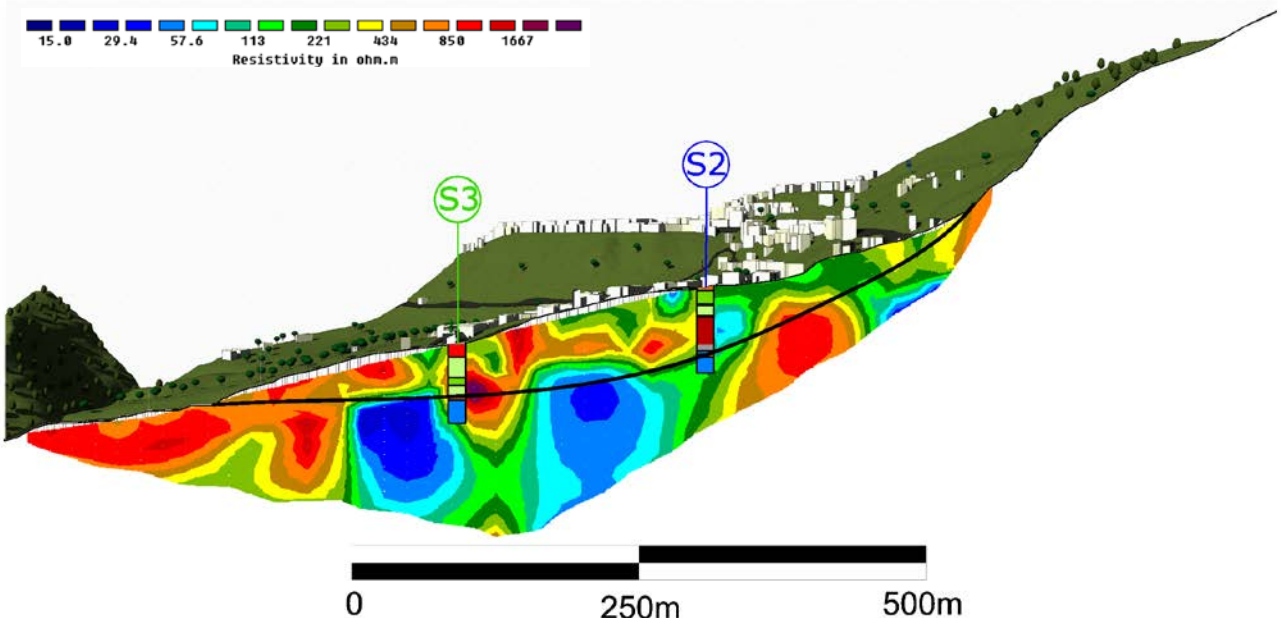

Figure 19. Final model of the Gimigliano landslide with the failure surface resulting from the combination of all presented data and measurements. In this sketch, stratigraphies for borings S2 and S3 are superimposed to a roughly co-located electrical resistivity tomography profile projected onto setion A-A' shown in Fig. 1.

5. References

Agnesi V., Camarda M., Conoscenti C., Di Maggio C., Serena Diliberto I., Madonia P., Rotigliano E. (2005) – *A multidisciplinary approach to the evaluation of the mechanism that triggered the Cerda landslide (Sicily, Italy)*. Geomorphology, 65, pp. 101–116.

Amodio-Morelli L., Bonardi G., Colonna V., Dietrich D., Giunta G., Ippolito F., Liguori V., Lorenzoni S., Paglionico A., Perrone V., Piccarreta G., Russo M., Scandone P., Zanettin-Lorenzoni E., Zuppetta A. (1976) – *L'arco Calabro-Peloritano nell'orogene appenninico Maghrebide (The Calabrian-Peloritan Arc in the Apennine-Maghrebide orogen)*. Memorie della Societa Geologica Italiana, 17, pp. 1–60.

ASTM (2008) – *ASTM D2845-08, Standard Test Method for Laboratory Determination of Pulse Velocities and Ultrasonic Elastic Constants of Rock (Withdrawn 2017)*. ASTM International, West Conshohocken, PA.

Ausilio E., Zimmaro P. (2014) – *A combined technique approach for the study of a landslide in the Calabria region*. Proc. of 20th IMEKO TC4 International Symposium and 18th International Workshop on ADC Modelling and Testing Research on Electric and Electronic Measurement for the Economic Upturn Benevento, Italy, September 15–17.

Ausilio E., Zimmaro P. (2017) – *Landslide characterization using a multidisciplinary approach*. Measurement, 104, pp. 294-301.

Basu A., Aydin A. (2006) – *Evaluation of ultrasonic testing in rock material characterization*. Geotech Test J, 29, n.2, pp. 117–125.

Bentivenga M., Bellanova J., Calamita G., Capece A., Cavalcante F., Gueguen E., Guglielmi P, Murgante B, Palladino G, Perrone A, Saganeiti L, Piscitelli S. (2021) – *Geomorphological and geophysical surveys with InSAR analysis applied to the Picerno earth flow (southern Apennines, Italy)*. Landslides, 18, n.1, pp. 471-483.

Bentivenga M., Giocoli A., Palladino G., Perrone A., Piscitelli S. (2019) – *Geological and geophysical characterization of the Brindisi di Montagna Scalo landslide (Basilicata, Southern Italy)*. Geomatics Nat Hazards Risk, 10, pp. 1367–1388.

Bianchini S., Cigna F., Del Ventisette C., Moretti S., Casagli N. (2013) – *Monitoring landslide-induced displacements with TerraSAR-X Persistent Scatterer Interferometry (PSI): Gimigliano case study in Calabria region (Italy).* Int J Geosci, 4, n.10, pp. 1467–1482.

Colonna V., Piccarreta G. (1975) – *Schema strutturale della Sila Piccola Meridionale (Structural scheme of the Southern Sila Piccola).* Bollettino della Societa Geologica Italiana, 94, pp. 3–16.

Colonna V., Piccarreta G. (1977) – *Carta geologico-petrografica della zona compresa tra Serra Stretta-Carlopoli-Gimigliano-Pianopoli (Sila Piccola, Calabria) (Geological-petrographic map of the area between Serra Stretta-Carlopoli-Gimigliano-Pianopoli (Sila Piccola, Calabria)).* Sviluppo 9, Arti Grafiche G. Favia, Bari, Italy.

Del Soldato M., Bianchini S., Calcaterra D., De Vita P., Di Martire D., Tomás R., Casagli N. (2017) – *A new approach for landslide-induced damage assessment*. Geomatics, Nat. Hazards Risk, 8, pp. 1524–1537.

Del Soldato M., Di Martire D., Bianchini S., Tomás R., De Vita P., Ramondini M., Casagli N., Calcaterra D. (2018) – *Assessment of landslide-induced damage to structures: The Agnone landslide case study (southern Italy).* Bull Eng Geol Environ, 78, pp. 2387–2408.

Filomena L. (2019) – *Ground displacements due to tectonics and gravity in Corace River Catchment. Gimigliano case study in Calabria Region (Italy).* Ph.D. Dissertation, University of Calabria, Italy.

Fortunato G., Ferrucci F. (2012) – *Interferometria satellitare, DEM ed analisi della dinamica altimetrica 1993–2010.* Technical Report, (in Italian).

Gaviglio P. (1989) – *Longitudinal waves propagation in a limestone: the relationship between velocity and density*. Rock Mechanics and Rock Engineering, 22, pp. 299-306.

Kahraman S. (2001) – *A correlation between P-wave velocity, numberof joints and Schmidt hammer rebound number*. Int J Rock Mech Min Sci, 38, pp.729–733.

Kahraman S., Soylemez M., Gunaydin O., Fener M. (2005) – *Determination of some physical properties of travertines frombultrasonic measurement*. Proc. of the First International Symposium on Travertine, Denizli, pp. 231–234.

Kahraman S., Yeken T. (2008) – *Determination of physical properties of carbonate rocks from P-wave velocity*. Bull Eng Geol Environ, 67, pp. 277–281.

Mantovani M., Devoto S., Forte E., Mocnik A., Pasuto A., Piacentini D., Soldati M. (2013) – *A multidisciplinary approach for rock spreading and block sliding investigation in the northwestern coast of Malta*. Landslides, 10, pp. 611–622.

Messina A., Russo S., Borghi A., Colonna V., Compagnoni R., Caggianelli A., Fornelli A., Piccarreta G. (1994) – *Il Massiccio della Sila, Settoresettentrionale dell'Arco Calabro-Peloritano (The Sila Massif, northern sector of the Calabrian-Peloritan Arc).* Bollettino della Societa Geologica Italiana. 113, pp. 539–586.

Notti D., Galve J.P., Mateos R.M., Monserrat O., Lamas-Fernández F., Fernández-Chacón F., Roldán-García F.J., Pérez-Peña J.V., Crosetto M., Azañón J.M. (2015) – H*uman-induced coastal landslide reactivation. Monitoring by PSInSAR techniques and urban damage survey (SE Spain).* Landslides, 12, pp. 1007–1014.

Ozkahraman H.T., Selver R., Isik E.C. (2004) – *Determination of the thermal conductivity of rock from P-wave velocity*. Int J RockbMech Min Sci, 41, pp. 703–708.

PAI (2016) – *Piano Stralcio di Bacino per l'Assetto Idrogeologico Regione Calabria*. Autorità di bacino Calabria, available at: http://old.regione.calabria.it/abr/index.php?option=com_content&task=view&id=504&Itemid=330. Last accessed January 1, 2021.

Pastor J.L., Tomás R., Lettieri L., Riquelme A., Cano M., Infante D., Ramondini M., Di Martire D. (2019) – *Multi-source data integration to investigate a deep-seated landslide affecting a bridge*. Remote Sensing, 11, n.16, 1878.

Rizzo E., Giocoli A., Piscitelli S., Romano G., Votta M. (2012) – *Tomografie geoelettriche ad alta risoluzione (ERT) per la caratterizzazione del versante in frana presso il Comune di Gimigliano (CZ)*. Technical Report (in Italian).

Rossetti F., Faccenna C., Goffe P., Monie P., Argentieri A., Funiciello R., Mattei M., 2001 – *Alpine structural and metamorphic segnature of the Sila Piccola Massif nappe stack (Calabria, Italy): insights for a tectonic evolution of the Calabrian Arc*. Tectonics, 20, n.1, pp. 112–133.

Sharma P.K., Singh T.N. (2008) – *A correlation between P-wave velocity, impact strength index, slake durability index and uniaxial strentgh*. Bull Eng Geol Environ, 67, pp. 17–22.

Straface S., De Luca D., Saraceni F. (2012) – *A-G6 – Idrologia, Idraulica e Idrogeologia*. Technical Report, (in Italian) in Studi ed indagini geologiche, geotecniche, idrologiche e idrauliche nel comune di Gimigliano.

Tansi C., Muto F., Critelli S., Iovine G. (2007) – *Neogene-Quaternary strike-slip tectonics in the central Calabrian Arc (southern Italy)*. Journal of Geodynamics, 43, pp. 393-414.

Tomás R., Abellán A., Cano M., Riquelme A., Tenza-Abril A. J., Baeza-Brotons F., Saval J.M, Jaboyedoff M. (2018) – *A multidisciplinary approach for the investigation of a rock spreading on an urban slope*. Landslides, 15, pp. 199-217.

Travelletti J., Malet J.P. (2012) – *Characterization of the 3d geometry of flow-like landslides: a methodology based on the integration of heterogeneous multi-source data*. Eng Geol, 128, pp. 30–48.

Yasar E., Erdogan Y. (2004) – *Correlating sound velocity with thedensity, compressive strength and Young's modulus of carbonate rocks*. Int J Rock Mech Min Sci, 41, pp. 871–875.

Zimmaro P., Stewart J.P. (2017) – *Site-specific seismic hazard analysis for Calabrian dam site using regionally customized seismic source and ground motion models*. Soil Dynamics and Earthquake Engineering, 94, pp. 179-192.